Macromolecules

Article

pubs.acs.org/Macromolecules

# Switching the Adhesive State of Catecholic Hydrogels using Phototitration

Evan M. White,[†] Jonathan E. Seppala,[‡] Parker M. Rushworth,[†] Branson W. Ritchie,[†] Suraj Sharma,[†] and Jason Locklin[†,*]

[†]Chemistry Department, The University of Georgia, 220 Riverbend Road, Athens, Georgia, 30602, United States

[‡]Materials Science and Engineering Division, National Institute of Standards and Technology, 100 Bureau Drive, Gaithersburg, Maryland, 20899, United States

Supporting Information

**ABSTRACT:** A polyacrylamide hydrogel system that can be liquefied by remote activation using UV irradiation is investigated as a degradable adhesive. The linear polyacrylamide copolymer, formed by conventional free-radical polymerization, contains biomimetic catechol–iron-mediated cross-linkers that are sensitive to pH changes. Hydrogel films and bulk gels are prepared by basic titration of a polymer solution doped with a photoacid generator, diphenyliodonium chloride, generating an ionic cross-linked network via the catechol pendant groups. Irradiation of these hydrogels with UV light affords a viscous liquid solution, demonstrating a gel–sol transition with a subsequent decrease in the adhesive strength of the material. These gels may be prepared in high throughput and require few synthetic steps with commercially available precursors.

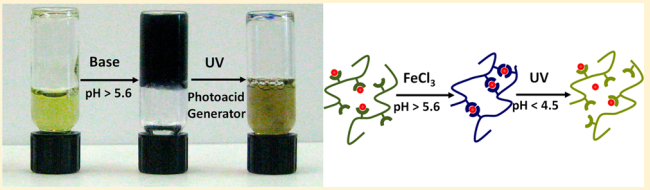


## INTRODUCTION

Hydrogels are found in nature as scaffolds for adhesive proteins such as those found in marine mussels in coastal regions.[1] The strong, aqueous adhesion of these particular proteins is attributed to the 3,4-dihydroxyphenylalanine (DOPA) residues that coordinatively bond to transition metal oxides on the surface of rocks. Much work has been accomplished to understand the adhesive properties of DOPA, which is found in high concentration in the mussel's adhesive plaques, and similar synthetic analogues.[1−12] Recent polymeric hydrogels containing DOPA analogues have produced a variety of novel devices that respond macroscopically to external stimuli, such as changes in pH[12−14] or light.[5,15] Some other smart hydrogels can respond to changes in ionic strength,[16,17] temperature,[18] mechanical stress,[14,19] enzymatic degradation,[20,21] and light, which is of particular interest because of remote activation.[5,15,22−30]

Among the many stimuli-responsive functions, developing a material that undergoes a sol-to-gel transition has been an attractive response behavior, which often operates on the dissolution or cross-linking of the polymeric network.[15,31−37] Such hydrogels are typically 90% or more by weight solvent and form gels from a prepolymer solution upon the application of a stimulus. The use of gels with switchable architectures, such as cross-linkers, has the potential to contribute added function to biodegradable adhesives, medical devices, and other smart materials. Furthermore, polymeric hydrogel systems constructed from acrylic monomers are commonly used commercially due to their ease of fabrication, biocompatibility, and low cost. Combining the use of biomimetic chemistry with acrylic polymers will advance adhesion science with dynamic bonding–debonding architectures.

This paper describes the development of a pH-dependent biomimetic hydrogel that can be switched to a liquid solution state upon irradiation with UV light (254 nm). These hydrogels are prepared post polymerization by cross-linking linear acrylic polymers with the addition of $NaHCO_3$ in the presence of pendant catechol groups and aqueous $Fe^{3+}$ above pH 5.6 through coordinative complexation. The iron-catechol complex is switchable, and may be uncross-linked in acidic conditions (Figure 1).[13]

This hydrogel system contains two stimuli-responsive components that operate concertedly under UV irradiation, resulting in a decrease in the overall cohesive strength of the material. The pH-sensitive DOPA analogue is complexed to aqueous iron through the bis-catechol cross-links by basic titration to pH 5.6–7.0.[12,14] The network accommodates a light-responsive photoacid generator, which functions as the remote trigger for acid production. As pH decreases within the gel upon UV irradiation, pH-sensitive cross-link points are dismantled and the hydrogel reverts to an aqueous solution. Herein, we investigated the photoinduced transformation of these systems, as bulk gels and solution cast films, from a gel to the resulting liquid polymer solution.

**Received:** July 29, 2013
**Revised:** October 15, 2013





dx.doi.org/10.1021/ma401594z | *Macromolecules* XXXX, XXX, XXX–XXX

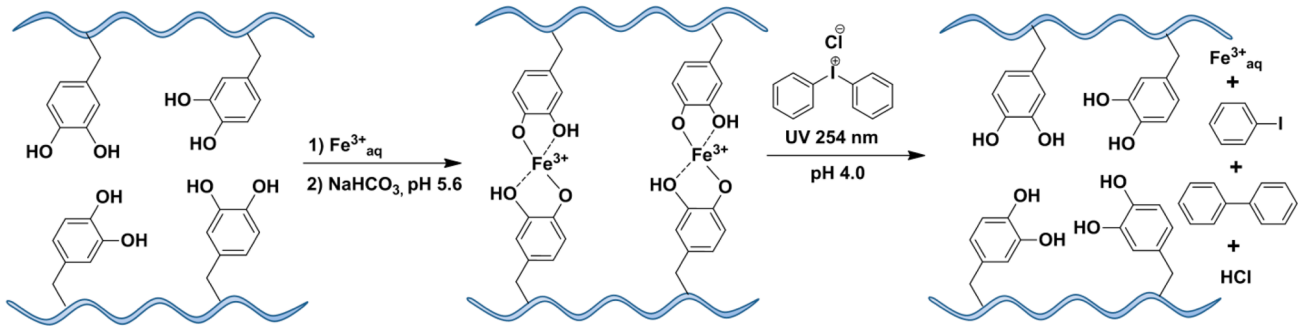


**Figure 1.** Formation of switchable hydrogels and photodegradation via the photoacid generator diphenyliodonium chloride. The iron-mediated bis-catechol complex (shown middle) may be dismantled by protonation of the ferric−phenoxide coordinative bond by photoinduced titration with the photoacid generator diphenyliodonium chloride.

## EXPERIMENTAL DETAILS

**Synthesis of *N*-(3,4-Dihydroxyphenethyl)methacrylamide Monomer Modified from Reference 10.** Synthesis and characterization of *N*-(3,4-dihydroxyphenethyl) methacrylamide (DMA) was synthesized in a similar fashion as previously reported.[10] To synthesize responsive DOPA monomer, 10.0 g of $Na_2B_4O_7$ (26.22 mmol) and 4.0 g of $NaHCO_3$ (47.61 mmol) were dissolved in 100 mL of 18 MΩ water, displaying some insolubility. This solution was degassed for 45 min with nitrogen, after which 5.0 g (32.64 mmol) of dopamine HCl was added to the mixture and allowed to stir under nitrogen atmosphere. A separate a solution of 4.7 mL (31.71 mmol) of methacrylic anhydride in 25 mL of degassed THF was prepared and added dropwise. The pH of the reaction mixture was monitored periodically with pH paper and maintained slightly basic (pH 8−9) by addition of degassed 1.0 M NaOH. Once all the methacrylic anhydride solution was added, the solution was allowed to stir for 17 h at room temperature, resulting in a light brown solution. This solution was washed with two 50 mL portions of ethyl acetate and the resulting aqueous layer was filtered. The filtrate was acidified to pH 2 with 6 M HCl. This mixture was extracted three times with 50 mL of ethyl acetate, dried with $MgSO_4$ and condensed down to approximately 20 mL under reduced pressure, and precipitated into 0 °C hexane. The white precipitate was collected and recrystallized from boiling ethyl acetate to afford white crystals collected by vacuum filtration and dried under vacuum in 82% isolatable yield. $^1$H NMR (300 MHz, DMSO-$d_6$, $\delta$): 8.740 (s, 1H, ArOH), 8.625 (s,1H, ArOH), 7.927 (t, $J$ = 5.4, 1H, NH), 6.630 (d, $J$ = 7.9, 1H, ArH), 6.578 (d, $J$ = 2.0, 1H,ArH), 6.439 (dd, $J_1$ = 7.9, $J_2$ = 2.0, 1H), 5.616 (t, $J$ = 1.5, 1H, $CH_2$), 5.304 (t, $J$ = 1.5, 1H,), 3.230 (q, $J$ = 6.0, 2H, $CH_2$), 2.554 (t, $J$ = 7.5, 2H, $CH_2$), 1.840 (s, 3H, $CH_3$).

**Synthesis of Poly(dopamine methacrylamide-*co*-*N*-isopropylacrylamide-*co*-acrylamide).** Acrylamide (1.479 g, 20.81 mmol), *N*-isopropylacrylamide (2.355 g, 20.81 mmol), *N*-(3,4-dihydroxyphenethyl) methacrylamide (0.252 g, 1.138 mmol), and azobis-(isobutyronitrile) (0.043 g, 0.263 mmol) were dissolved in a Schlenk flask with 10 mL DMSO and degassed for 2 h with argon sparging at room temperature. The solution was then placed in an oil bath thermostated to 60 °C for 25 min, at which point the solution reaches the gel point. The solution was then quenched by cooling to 0 °C and addition of 40 mL air-free $H_2O$. This mixture was sonicated and stirred vigorously under nitrogen to redissolve the gel. In a nitrogen glovebox, this solution was then washed thrice with 50 mL of degassed dichloromethane and washed once with 50 mL of chloroform. The resulting aqueous layer was precipitated into 50:50 2-propanol:hexane mixture with vigorous stirring resulting in a white, tough, and sticky solid. The polymer was collected by decanting and dried under reduced pressure overnight with an isolatable yield of 82%. The weight-average molecular weight ($M_w$) was determined to be 904 kg/mol by dynamic light scattering (DLS) as shown in Figure S2. The percent catechol retention, $\chi$, of the polymer is determined by the NMR molar ratio, $\sigma$, and the molar feed ratio, $N$, of DMA/NIPAM monomers by eq 1:

$$\chi = \frac{\sigma}{N} \tag{1}$$

Here $\sigma$ is determined by integrals of the NIPAM proton and two phenolic protons of DMA, $\Sigma_{NIPAM}$ and $\Sigma_{DMA}$, respectively, by eq 2:

$$\sigma = \frac{\frac{\Sigma_{DMA}}{2H}}{\frac{\Sigma_{NIPAM}}{1H}} \times 100\% \tag{2}$$

All polymer batches prepared at 2.66 mol % DMA retained greater than 97% catechol functionality.

**Preparation of Hydrogels at 1.6% by Mass.** Dry, native prepolymer p(DMA-*co*-NIPAM-*co*-AcAm) is first dissolved at 20 mg·mL$^{-1}$ with previously degassed water, 5.58 mM DMA content (3 equiv). Once the polymer dissolved, 21 mg·mL$^{-1}$ of diphenyliodonium chloride (35.7 equiv) was dissolved in the solution with sonication. Then, 1.00 mL of this solution was mixed with 65 $\mu$L of 28.42 mM $FeCl_3$ (1 equiv), in a cylindrical mold 0.45 cm high and 2.25 cm in diameter. After that, 200 $\mu$L of 28.42 mM $NaHCO_3$ (3 equiv) was then mixed aggressively into this solution using a spatula, generating a purple gel which was allowed to cure for 10 min covered with a quartz cover slide to prevent evaporation. Thin film gels were prepared in the same fashion except in 75 $\mu$L polymer solution volumes, spread over 645 mm$^2$ area on a quartz slide. Subsequently, 15 mg of 28.42 mM $NaHCO_3$ was then added to the polymer solution by spraying through an aluminum shadow mask to form the gel, at which point the quartz slides are affixed to cure for 10 min. The gels were then irradiated with 254 nm light from a hand-held UV lamp at a distance of 2 cm for 30 min for bulk gels and 60 s for thin films. Certain commercial equipment, instruments, or materials are identified in this paper in order to specify the experimental procedure adequately. Such identification is not intended to imply recommendation or endorsement by the National Institute of Standards and Technology, nor is it intended to imply that the materials or equipment identified are necessarily the best available for the purpose. The error bars represent one standard deviation of the data, which is taken as the uncertainty of the measurement.

## RESULTS

Synthesis of p(DMA-*co*-NIPAM-*co*-AcAm) hydrogel prepolymer was prepared by conventional free radical polymerization of the corresponding acrylamide monomers in DMSO using 2,2′-azobis(isobutyronitrile) (AIBN) as an initiator (see Supporting Information for experimental details). Catechol groups are often protected with alkyl silanes,[13] nitrobenzyl,[15] or boronic esters,[38] which prevents oxidation; however, by limiting the polymerization reaction time, increasing monomer concentration, and employing oxygen-free work up protocols, the hydrogel prepolymer was prepared in modest isolatable yields (82%), with a high retention of the catechol group, (97% by NMR, Figure S1) without the use of protection chemistry.


dx.doi.org/10.1021/ma401594z | *Macromolecules* XXXX, XXX, XXX−XXX

In lieu of aqueous GPC, the polymer's weight-average molecular weight, $M_w$, was determined to be approximately 904 kDa by dynamic light scattering (Figure S2). The native hydrogel prepolymer solutions were prepared and stored in degassed water prior to use.

**Preparation and Characterization of Hydrogels at 1.6% by Mass.** Previous work by Messersmith and Deming have shown that the catechol groups will irreversible oxidize to the quinone under basic conditions in the absence of iron.[2,39] Addition of aqueous iron to the optimal ratio of 1:3 = $Fe^{3+}$:catechol (Figure S8) was used for these gels as described in earlier work by the del Campo and Takahara groups.[5,13] As the polymer solution is titrated from acidic to more basic pH, there is a distinct increase in viscosity due to the formation of catechol-coordinated ferric ions acting as cross-linkers, along with a discrete colorimetric response (Figure 2).

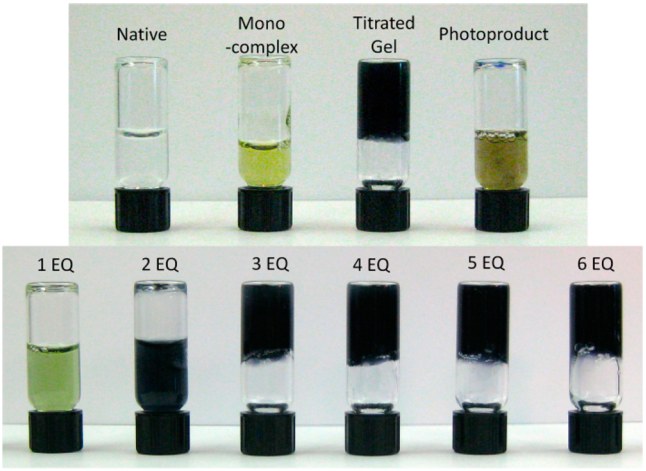


**Figure 2.** Photograph of bulk hydrogels prepared at 1.6% by mass in water. Top: from left to right showing the native polymer solution, monocomplex, titrated gel, and photoproduct. Bottom: demonstrating gel performance and transition about sol–gel point with 1 equiv of $NaHCO_3$ (pH 4.7) to 6 equiv (pH 7.0).

For bulk gel preparation, 1 mL of 20 mg·mL$^{-1}$ aqueous, air-free solution of p(DMA-*co*-NIPAM-*co*-AcAm) with 5.58 mM DMA content (3 equiv) doped with 21 mg·mL$^{-1}$ diphenyliodonium chloride (35.7 equiv, 66 mM) was combined with 65 $\mu$L of 28.42 mM $FeCl_3$ (pH 3.9), generating the green solution of monocomplexed iron-catechol coordinative pendant groups. Titrating the solution to pH 5.6–5.7 (3 equiv of $NaHCO_3$) resulted in a purple gel. Although a strong base like NaOH can be used to induce gelation, the use of the weaker base slowed the rate of gel formation and allowed for a more consistent and uniform gel. Titrating the solution to a ratio of 3:1:3 = DMA:$Fe^{3+}$:$NaHCO_3$ brings the pH over 5.6 and populates the mixture with the bis-complex cross-linkers and gels the solution. Once gelled, the solution may be irradiated with 254 nm light to generate HCl *in situ* and subsequently uncross-link the gel to form a viscous polymer solution.

**Characterization of Iron(III) Complexation by UV–Vis Spectroscopy.** The sol–gel transition is observed upon the addition of 3 equiv of $NaHCO_3$ relative to the catechol groups with gels prepared at 1.6% by mass (Figure 2). The colorless native hydrogel prepolymer solution is acidified by the addition of ferric chloride, and catechol complexation was observed by UV–vis spectroscopy through the evolution of a green-yellow solution (Figure S3), with a shoulder peak near 400 nm and a broad peak centered at 710 nm (Figure 3). As the

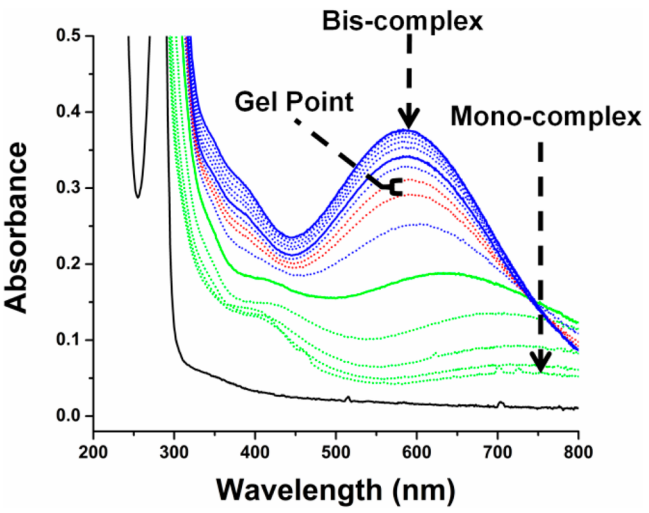


**Figure 3.** Solid black line representing the native catechol polymer in solution at 2 mg·mL$^{-1}$. Green lines represent the addition of 2.0 equiv of $NaHCO_3$ relative to $Fe^{3+}$ at 0.4 equiv increments (from pH 4.1 to 5.2). The two solid blue lines represent the addition of 4 and 6 equiv of $NaHCO_3$ at pH 6.4 and 7.0, respectively. Red lines represent the gel point pH 5.5–5.6.

monocomplex solution is titrated with $NaHCO_3$ above pH 5.6, the onset of bis-complex formation is observed by the broad peak centered at 750 nm (Figure 3). The decrease in the absorbance at 750 nm and the decrease of the shoulder peak at 400 nm suggest the loss of monocomplexed polymer upon the addition of 6 equiv of $NaHCO_3$ (pH = 7.0), and mostly the presence of the bis-complex, $\lambda_{max}$ = 585 nm.

As the pH increases from 4.1 to 5.2 (green lines), the iron–catechol monocomplex peak displays a hypsochromic shift and, the bis-complex dominates over the monocomplex. Further titrating the gel with sodium bicarbonate to pH 5.5–5.6 (red lines) will create a sufficient concentration of cross-link points to form a 1.6% by mass gel. Increasing the pH from 5.6–7.0 (blue lines) further cross-links the gel; however, in this system, we aimed to generate a gel just over the sol–gel transition, such that subtle variations in pH would influence a macroscopic transition.

In order to evaluate the phototitration efficacy, a 1.6% by mass solution of pDMA-*co*-NIPAM-*co*-AcAm was prepared with 3 equiv of $NaHCO_3$ relative to ferric ions and was irradiated with 254 nm UV light at 0.22 mW·cm$^{-2}$ (Figure 4). The peak at 585 nm representing the bis-complex disappears after approximately 25 min of UV exposure. The molar extinction coefficients for diphenyliodonium chloride and the bis-complex at 253.9 nm were measured to be 5160 and 2110 M$^{-1}$·cm$^{-1}$ respectively (Figure S4).

The polymer was prepared at 1 mg·mL$^{-1}$ (0.28 mM DMA content) concentrations with 3.32 mM, 0.332 mM, and 0.033 mM (35.7equiv, 3.57 equiv and 0.36 equiv respectively) diphenyliodonium chloride concentrations for UV–vis studies in order to investigate the time dependence of the system on photoacid concentration and the minimum photoacid required to reduce the catechol cross-links. Figures S11 and S12 show the corresponding $NaHCO_3$ titration data with in situ UV–vis data and subsequent phototitration for 300 s (20 s exposure


dx.doi.org/10.1021/ma401594z | *Macromolecules* XXXX, XXX, XXX–XXX

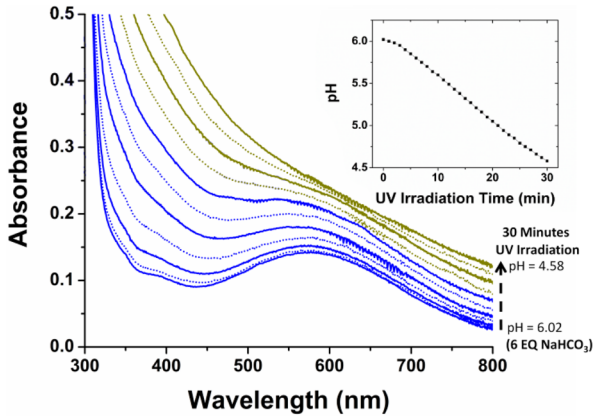


**Figure 4.** UV−vis spectra of a 2 mg·mL$^{-1}$ pDMA solution first titrated to pH 6.02 with $NaHCO_3$ and subsequent irradiation for 30 min at 0.22 mW·cm$^{-2}$. The inset is the corresponding titration curve. The overall increase in spectral absorbance is due to light scattering of immiscible photoproducts. Solid lines correspond to 6 min intervals of UV exposure.

intervals) at these concentrations. Phototitration of the bis-complex down to pH 4.6 was observed to occur in 300 and 180 s in the case of the 0.332 mM and 3.32 mM diphenyliodonium chloride experiments respectively, but the bis-complex remained at pH 5.4 at 0.033 mM photoacid generator after 300 s exposure. At pH 4.6, an equivalence point was observed (Figure S5), suggesting that not all ferric ions are dissociated, rather there is a distribution of monocomplexed and protonated catechol groups below pH 4.6.

The concentration of the photoacid generator is 12 times larger than the DMA complex; therefore, the majority of the UV light is absorbed by the diphenyliodonium chloride rather than the DMA pendant groups. Production of HCl from photoacid action under UV light titrates the gel to approximately pH 4.6, reducing the bis-complex cross-linker to a mixture of the monocomplex and protonated catechol moiety, effectively liquefying the gel to a solution (Figure S5). Irradiation of the control experiment with no photoacid generator present shows no significant change in bis-complex concentration or in pH (Figure S10).

Since only the bis-complex is associated with cross-linking, changes in the concentration of the monocomplex do not change molecular weight between cross-links. It is important to note that the spectra in Figure 4 show an increase in scattering with time at longer wavelengths, which presumably occurs through irreversible cross-linking of the polymer backbone (Figure S6 and S12). This photoproduct is confined as a film on the UV−solution interface, and was easily discarded for reproducible mechanical analysis. Furthermore, the use of a photoacid generator that absorbs at lower energy wavelengths would reduce the formation of the insoluble photoproducts.

**Mechanical Analysis of Hydrogels.** Hydrogels were prepared as both bulk gels and films, depending on the analysis technique. The response time for liquefaction of 0.45 cm thick bulk hydrogels is on the order of minutes (Figure S7) to complete the phototitration, while thin films are liquefied in 60 s. The bulk hydrogels were prepared at 1.6% by mass for analysis via small amplitude oscillatory shear (SAOS) to investigate the gel and sol material properties (Figure 5).

The pre-UV hydrogel exhibits a typical cross-linked material response where the storage modulus ($G'$) is greater than the loss modulus ($G''$), and the material exhibits shear thickening at high strain amplitude. After UV irradiation, the loss modulus dominates ($G'' > G'$) and the material exhibits slight shear thinning, typical of polymer solutions, demonstrating the material has transitions from gel to sol. Evidence of this transition by rheological data helps support that the mechanism for liquefaction is acidic titration of the iron−catechol bis-complex.

For thin film preparation, the hydrogel is prepared in the same manner as for bulk gels except in 75 $\mu$L volumes spread over one square inch area (645 mm$^2$) on two quartz slides. To evenly distribute base, the monocomplex prepolymer solution was titrated gravimetrically by adding approximately 15 mg of 28.42 mM $NaHCO_3$ (3 equiv) by spraying through an aluminum shadow mask. Immediately after introducing the base, the gel film turned purple in color, and a second quartz slide was affixed to the gel to cure for 10 min (Figure S6).

The gels are prepared as films to expedite the reaction time because UV exposure is limited to the gel interface; therefore, acid titration of the cross-link points is assumed to be a diffusion limited process from that interface. The adhesive properties of the gel were analyzed by lap-shear adhesion testing on an Instron tensile tester using a 1.27 mm/min displacement rate. Upon exposure to 60 s of 254 nm UV light at a distance of approximately 2 cm (1.20 mW·cm$^{-2}$), the adhesive film's maximum tensile shear strength dropped from 1.68 kPa before irradiation to 0.35 kPa after irradiation (Figure 6). In both experiments, before and after UV exposure, the gel fails cohesively, implying a network failure, rather than adhesive debonding. A time-lapse video of the debonding event in which the substrate supports a 20 g load is shown in the Supporting Information.

Similar to the SAOS measurements a large decrease in adhesion strength is observed between the gels before and after

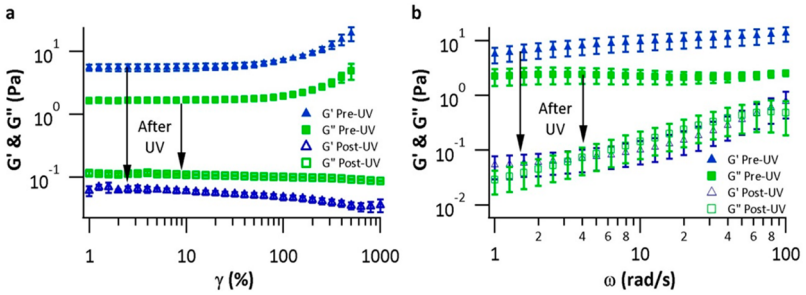


**Figure 5.** (a) Isothermal strain sweeps and (b) isothermal frequency sweeps of 1.6% by mass hydrogels prepared at 3:1:3 = DMA:$Fe^{3+}$:$NaHCO_3$ (pH 5.6) before and after UV irradiation with 254 nm light. Error bars indicate first standard deviation from five independent samples.


dx.doi.org/10.1021/ma401594z | Macromolecules XXXX, XXX, XXX−XXX

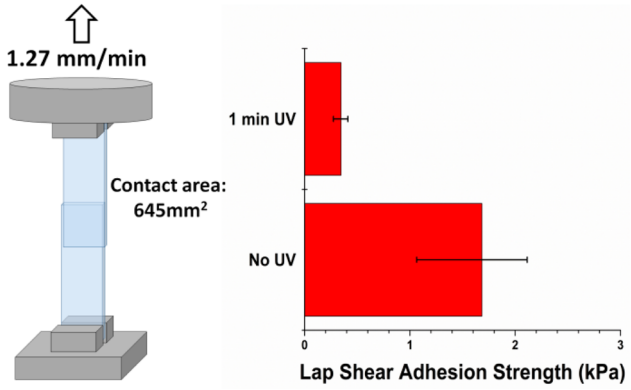


**Figure 6.** Lap shear adhesive strength testing of a 1.6% by mass p(DMA-*co*-NIPAM-*co*-AcAm) hydrogel before and after UV irradiation at 1.2 mW·cm$^{-2}$. Error bars represent the first standard deviation from 8 independent samples.

UV irradiation, suggesting that the network of catechol cross-links is dismantled as the pH decreases. Earlier work by the Messersmith group showed that the breaking force of a metal-catechol bond is a modest 0.8 nN of force compared to a covalent bond which requires 2−3 nN of force to rupture,[2] and more recent work by Zhiping attests to the high bond strength (approximately 6 nN) required to rupture the ferric−catechol bis-complex by DFT calculations.[40] We speculate that the onset of bis-complex formation at pH 5.6 observed by UV−vis develops a minimum population of bis-complex cross-linkers with sufficient mechanical strength to gel the solution. Titrating the hydrogel about this ratio gives the most dramatic changes in cohesive mechanical strength at small changes in pH.

## CONCLUSION

Acrylic copolymer hydrogels offer an attractive approach for the development of smart hydrogels due to their ease of fabrication and commercially available starting materials. We have designed a biomimetic catechol-based hydrogel that may be remotely activated to photodegrade back into a sol, displaying a decrease in the modulus and lap shear adhesion strength of the material. Hydrogels prepared in this fashion at pH 5.6−6.0 supplies the hydrogel with bis-complex cross-links, demonstrating a sol−gel transition which may be titrated back to a solution with a decrease in pH. This hydrogel incorporates two cooperative systems, a photoacid generator and a pH-responsive cross-linker. Currently we are exploring the use of photobase generators in efforts to develop a material capable of undergoing sol−gel transitions without the constraints of added mass.

## ASSOCIATED CONTENT

### Supporting Information

Synthesis and preparation of hydrogels, $^1$H NMR, DLS, titration data, FTIR, UV−vis characterization, and rheological techniques and a time-lapse video of the debonding event. This material is available free of charge via the Internet at http://pubs.acs.org.

## AUTHOR INFORMATION

### Corresponding Author

*E-mail: (J.L.) jlocklin@uga.edu.

### Notes

The authors declare no competing financial interest.



## ACKNOWLEDGMENTS

We gratefully acknowledge financial support from the National Science Foundation (CAREER Award, DMR 0953112).

## REFERENCES

(1) Waite, J. H. *Nat. Mater.* **2008**, *7*, 8−9.
(2) Lee, H.; Scherer, N. F.; Messersmith, P. B. *Proc. Natl. Acad. Sci. U.S.A.* **2006**, *103*, 12999−13003.
(3) Lee, H.; Dellatore, S. M.; Miller, W. M.; Messersmith, P. B. *Science* **2007**, *318*, 426−430.
(4) White, J. D.; Wilker, J. J. *Macromolecules* **2011**, *44*, 5085−5088.
(5) Shafiq, Z.; Cui, J.; Pastor-Pérez, L.; San Miguel, V.; Gropeanu, R.; Serrano, C.; del Campo, A. *Angew. Chem., Int. Ed.* **2012**, *51*, 4332−4335.
(6) Yamada, K.; Aoki, T.; Ikeda, N.; Hirata, M. *J. Appl. Polym. Sci.* **2007**, *104*, 1818−1827.
(7) Monahan, J.; Wilker, J. J. *Langmuir* **2004**, *20*, 3724−3729.
(8) Lee, B. P.; Messersmith, P. B.; Israelachvili, J. N.; Waite, J. H. *Annu. Rev. Mater. Res.* **2011**, *41*, 99−132.
(9) Chirdon, W. M.; O'Brien, W. J.; Robertson, R. E. *J. Biomed. Mater. Res. B.* **2003**, *66B*, 532−538.
(10) Glass, P.; Chung, H.; Washburn, N. R.; Sitti, M. *Langmuir* **2009**, *25*, 6607−6612.
(11) Brooksby, P. A.; Schiel, D. R.; Abell, A. D. *Langmuir* **2008**, *24*, 9074−9081.
(12) Holten-Andersen, N.; Harrington, M. J.; Birkedal, H.; Lee, B. P.; Messersmith, P. B.; Lee, K. Y. C.; Waite, J. H. *Proc. Natl. Acad. Sci. USA.* **2011**, *108*, 2651−2655.
(13) Xu, H.; Nishida, J.; Ma, W.; Wu, H.; Kobayashi, M.; Otsuka, H.; Takahara, A. *ACS Macro Lett.* **2012**, *1*, 457−460.
(14) Krogsgaard, M.; Behrens, M. A.; Pedersen, J. S.; Birkedal, H. *Biomacromolecules* **2013**, *14*, 297−301.
(15) Nishida, J.; Kobayashi, M.; Takahara, A. *ACS Macro Lett.* **2013**, *2*, 112−115.
(16) Bassik, N.; Abebe, B. T.; Laflin, K. E.; Gracias, D. H. *Polymer* **2010**, *51*, 6093−6098.
(17) Thérien-Aubin, H.; Wu, Z. L.; Nie, Z.; Kumacheva, E. *J. Am. Chem. Soc.* **2013**, *135*, 4834−4839.
(18) Hu, J.; Liu, S. *Macromolecules* **2010**, *43*, 8315−8330.
(19) Haque, M. A.; Kurokawa, T.; Kamita, G.; Yue, Y.; Gong, J. P. *Chem. Mater.* **2011**, *23*, 5200−5207.
(20) Vemula, P. K.; Cruikshank, G. A.; Karp, J. M.; John, G. *Biomaterials* **2009**, *30*, 383−393.
(21) van Bommel, K. J. C.; Stuart, M. C. A.; Feringa, B. L.; van Esch, J. *Org. Biomol. Chem.* **2005**, *3*, 2917−2920.
(22) Ercole, F.; Thissen, H.; Tsang, K.; Evans, R. A.; Forsythe, J. S. *Macromolecules* **2012**, *45*, 8387−8400.
(23) Kim, S.-H.; Hwang, I.-J.; Gwon, S.-Y.; Son, Y.-A. *Dyes Pigm.* **2010**, *87*, 158−163.
(24) Szilágyi, A.; Sumaru, K.; Sugiura, S.; Takagi, T.; Shinbo, T.; Zrínyi, M.; Kanamori, T. *Chem. Mater.* **2007**, *19*, 2730−2732.
(25) Kloxin, A. M.; Kasko, A. M.; Salinas, C. N.; Anseth, K. S. *Science* **2009**, *324*, 59−63.
(26) Tibbitt, M. W.; Anseth, K. S. *Biotechnol. Bioeng.* **2009**, *103*, 655−663.
(27) Tibbitt, M. W.; Kloxin, A. M.; Dyamenahalli, K. U.; Anseth, K. S. *Soft Matter* **2010**, *6*, 5100−5108.
(28) Tibbitt, M. W.; Kloxin, A. M.; Sawicki, L. A.; Anseth, K. S. *Macromolecules* **2013**, *46*, 2785−2792.
(29) White, E. M.; Yatvin, J.; Grubbs, J. B.; Bilbrey, J. A.; Locklin, J. *J. Polym. Sci., Polym. Phys.* **2013**, *51*, 1084−1099.
(30) Wang, E.; Desai, M. S.; Lee, S.-W. *Nano Lett.* **2013**, *13*, 2826−2830.
(31) Yang, Z.; Gu, H.; Fu, D.; Gao, P.; Lam, J. K.; Xu, B. *Adv. Mater.* **2004**, *16*, 1440−1444.

(32) Yang, Z.; Liang, G.; Wang, L.; Xu, B. *J. Am. Chem. Soc.* **2006**, *128*, 3038−3043.
(33) Toledano, S.; Williams, R. J.; Jayawarna, V.; Ulijn, R. V. *J. Am. Chem. Soc.* **2006**, *128*, 1070−1071.
(34) Vemula, P. K.; Li, J.; John, G. *J. Am. Chem. Soc.* **2006**, *128*, 8932−8938.
(35) Williams, R. J.; Smith, A. M.; Collins, R.; Hodson, N.; Das, A. K.; Ulijn, R. V. *Nat. Nanotechnol.* **2009**, *4*, 19−24.
(36) Yang, Z.; Ma, M.; Xu, B. *Soft Matter* **2009**, *5*, 2546−2548.
(37) Ryu, J. H.; Lee, Y.; Kong, W. H.; Kim, T. G.; Park, T. G.; Lee, H. *Biomacromolecules* **2011**, *12*, 2653−2659.
(38) Su, J.; Chen, F.; Cryns, V. L.; Messersmith, P. B. *J. Am. Chem. Soc.* **2011**, *133*, 11850−11853.
(39) Yu, M.; Hwang, J.; Deming, T. J. *J. Am. Chem. Soc.* **1999**, *121*, 5825−5826.
(40) Zhiping, X. *Sci. Rep.* **2013**, *3*, 2914.